CT-based radiomics analysis of consolidation characteristics in differentiating pulmonary disease of non-tuberculous mycobacterium from pulmonary tuberculosis

QINGHU YAN[1], WENLONG ZHAO[1], HAILI KONG[1], JINGYU CHI[1], ZHENGJUN DAI[2], DEXIN YU[3] and JIA CUI[1]

[1]Department of Radiology, Shandong Public Health Clinical Center, Shandong University, Jinan, Shandong 250013; [2]Huiying Medical Technology (Beijing) Co., Ltd., Beijing 100192; [3]Department of Radiology, Qilu Hospital of Shandong University, Jinan, Shandong 250012, P.R. China

Received June 28, 2023; Accepted November 2, 2023

DOI: 10.3892/etm.2024.12400

Abstract. Global incidence rate of non-tuberculous mycobacteria (NTM) pulmonary disease has been increasing rapidly. In some countries and regions, its incidence rate is higher than that of tuberculosis. It is easily confused with tuberculosis. The topic of this study is to identify two diseases using CT radioomics. The aim in the present study was to investigate the value of CT-based radiomics to analyze consolidation features in differentiation of non-tuberculous mycobacteria (NTM) from pulmonary tuberculosis (TB). A total of 156 patients (75 with NTM pulmonary disease and 81 with TB) exhibiting consolidation characteristics in Shandong Public Health Clinical Center were retrospectively analyzed. Subsequently, 305 regions of interest of CT consolidation were outlined. Using a random number generated via a computer, 70 and 30% of consolidations were allocated to the training and the validation cohort, respectively. By means of variance threshold, when investigating the effective radiomics features, SelectKBest and the least absolute shrinkage and selection operator regression method were employed for feature selection and combined to calculate the radiomics score. K-nearest neighbor (KNN), support vector machine (SVM) and logistic regression (LR) were used to analyze effective radiomics features. A total of 18 patients with NTM pulmonary disease and 18 with TB possessing consolidation characteristics in Jinan Infectious Disease Hospital were collected for external validation of the model. A total of three methods was used in the selection of 52 optimal features. For KNN, the area under the curve (AUC; sensitivity, specificity) for the training and validation cohorts were 0.98 (0.93, 0.94) and 0.90 (0.88, 083), respectively; for SVM, AUC was 0.99 (0.96, 0.96) and 0.92 (0.86, 0.85) and for LR, AUC was 0.99 (0.97, 0.97) and 0.89 (0.88, 0.85). In the external validation cohort, AUC values of models were all >0.84 and LR classifier exhibited the most significant precision, recall and F1 score (0.87, 0.94 and 0.88, respectively). LR classifier possessed the best performance in differentiating diseases. Therefore, CT-based radiomics analysis of consolidation features may distinguish NTM pulmonary disease from TB.

Correspondence to: Dr Jia Cui, Department of Radiology, Shandong Public Health Clinical Center, Shandong University, 46 Lishan Road, Jinan, Shandong 250013, P.R. China
E-mail: 584872500@qq.com

Key words: radiomics, consolidation, CT, non-tuberculous mycobacteria, pulmonary tuberculosis

Introduction

Global incidence rate of non-tuberculous mycobacteria (NTM) pulmonary disease has been increasing rapidly (1,2). In the United States, the infection rate and prevalence of NTM exceed those of tuberculosis (TB) (3-5). NTM pulmonary disease is globally prevalent. NTM is currently a key public health problem (6). The growth of NTM is slower than that of pulmonary TB, making the disease course longer. Further, the overall cure rate is low due to resistance to first-line anti-TB drugs. NTM predominantly affects the lungs (7), with patients exhibiting chronic basic diseases and low immunity being more susceptible to NTM pulmonary disease. The imaging manifestations and clinical features of NTM are similar to TB, resulting in a high rate of misdiagnosis (7). If patients with NTM pulmonary disease are treated for TB, the treatment opportunity will be delayed (8). Sputum mycobacterium culture and strain identification are currently the primary methods employed to distinguish NTM pulmonary disease from TB. However, both methods are time-consuming, arduous and require strict laboratory standards (9). Additionally, the identification of strains is dependent upon a positive sputum mycobacterium culture, which poses a diagnostic challenge. However, the employment of computed tomography (CT) offers advantages, including rapid imaging, widespread availability and high-resolution density, thereby enabling feasible discrimination between diseases (10). Despite the advantages of CT, due to the high similarity of the pathogenesis and pathological features of NTM and TB, there is no reliable image feature to distinguish them (11). Consolidation is a common and

important CT feature of NTM and TB (12). Consolidation characteristics of the diseases are similar, making it difficult to distinguish with the naked eye. CT-based radiomics has exhibited potential in the diagnosis and differentiation of pulmonary diseases through high-throughput extraction and mining data features (13,14). Due to differences in pathology between these two diseases (15), the possibility of identifying the diseases is further enhanced. In the present study, the value of CT-based radiomics analysis of consolidation characteristics in differentiation of NTM pulmonary disease from TB was investigated. The present study aimed to establish an effective classifier to provide a novel simple diagnosis method for NTM and TB.

Materials and methods

Patient population and ethical approval. The present study was approved by Shandong Public Health Clinical Center (Shandong Provincial Chest Hospital) Ethics Committee and the requirement for consent for this retrospective analysis was waived (approval no. 2019XKYYEC-29). Subsequently, 89 patients with NTM pulmonary disease and 104 with TB undergoing CT imaging in the Shandong Public Health Clinical Center between January 2013 and July 2018 were retrospectively analyzed. At the same time, 27 patients with NTM pulmonary disease and 30 with TB undergoing CT imaging in the Jinan Infectious Disease Hospital (Jinan, China) were also collected for the external validation of the model. All patients with NTM pulmonary disease were diagnosed twice using sputum culture and strains were identified as the same pathogenic bacteria (16,17). All patients with TB were identified using TB diagnosis and classification standard' issued by the China National Health Service Commission on November 9th, 2017 (18). The sputum smears of each patient was positive for acid-fast bacilli at least once and was identified as *Mycobacterium tuberculosis* complex using the colloidal gold method (19). The inclusion criteria were as follows: i) Clinical symptoms upon laboratory examination or imaging consistent with TB infection; ii) CT images of the lung window and mediastinal window exhibited consolidation and iii) treatment was effective. Exclusion criteria were as follows: i) No consolidation features in CT images; ii) CT images displayed motion artifacts, poor image quality, large differences in scanning conditions or inconsistent layer thickness; iii) clinical suspicion of mixed infection and iv) presence of non-infectious disease with similar presentation. Based on these criteria, 11 patients with NTM pulmonary disease and 23 with TB were excluded, leaving a total of 75 patients with NTM pulmonary disease, including 46 males and 29 females (mean age, 57.1±13.5 years; range 23-86 years), and 81 with TB, including 53 males and 28 females (mean age, 45.4±18.7 years; range, 17-90 years).

CT examination. All patients whose lungs had been affected underwent a plain chest scan using a Philips 64-slice spiral CT scanner (Philips Ingenuity) before treatment and quality correction standards were met prior to the CT scan. The patients were in the supine posture and underwent a scan extending from lung apices to the upper abdomen, with imaging acquisition commencing 5 cm inferior to the diaphragmatic dome at maximum inhalation. The CT scanning parameters were as follows: Diameter of the inspected detector, 64.000x0.625 mm; the rotation time was 0.5 sec; the pitch, 1.375; the tube voltage was 120 kV; the tube current was 250-400 mA, which was modulated using an automatic tube current; Field of view (FOV), 35-40 cm; matrix was 512x512 thickness of the slice, 5 mm.

Image pre-processing, segmentation and extraction of radiomics features. All images were uploaded to Radiance's Radcloud platform V7.9 *mics.huiyihuiying.com* (Huiying Medical Technology Co., Ltd.) for further study. A total of two radiologists (10 and 25 years of experience) with expertise in chest disease assessed and delineated the consolidations in the lung window CT images (Window Width 1500, Window Level-500). The radiologists were blinded to clinical information. The radiologists delineated the outline of the consolidation on all contiguous slices by manually sketching the region of interest (ROI), with the contour line in close proximity to the outer edge of the consolidation. The ROI entirely encompassed the consolidation. If the consolidation was close to the mediastinum, chest wall and diaphragm, the radiologists drew 1 mm along the outside of the contour of the mediastinum, chest wall and diaphragm to avoid delineating the non-consolidation. The halo caused by the surrounding exudation was not included. Finally, a senior radiologist reassessed all ROIs. If the difference was ≥5%, the senior radiologist determined the boundary of the ROI (20).

Radiomic feature extraction and selection. Using Radcloud platform, 1,409 radiomics quantitative image features were extracted from the CT images. The functions were classified into four groups. The first group (first-order statistics) comprised 18 features that quantitatively described the distribution of voxel intensity in the CT images through common and basic indicators. The second group (features based on shape and size) contained 14 three-dimensional features that reflected the shape and size of the area. The third group (texture features) consisted of grey level run-length and co-occurrence texture matrices and size zone matrix and neighboring gray tone difference and gray level dependence matrix. The fourth group (1,302 features through 14 filters) were exponential, square, square root, logarithm, gradient, local binary patterns-2D and wavelets [low-high-low (LHL), low-high-high (LHH), high-low-low (HLL), (LLH), high-low-high (HLH), high-high-high (HHH), high-high-low (HHL), and low-low-low (LLL)].

To enhance the model reliability and decrease the feature dimension, three methods were used. Variance threshold was used to remove features with variance <0.8. Secondly, the k-best method (21) was employed to remove features with P-value >0.05. To establish a more refined model, the least absolute shrinkage and selection operator (LASSO, version 1.0.2) algorithm was used to formulate a penalty function to compress select regression coefficients (22). It includes three steps: LASSO path, mean Square Error path and coefficients in LASSO model. These steps were performed 50 times in the case of random initialization. Finally, the most frequent fixed features were selected for modeling.

Statistical analysis. Based on the selected features, numerous supervised learning classifiers were used for classification (version 7.9, Huiying Medical Technology Co., Ltd.) analysis (23). Three supervised learning models were employed in the present study: K-nearest neighbor (KNN), support vector machine (SVM) and logistic regression (LR). KNN is a basic classification and regression method (24). SVM is a generalized linear classifier for binary classification of data according to supervised learning, with decision boundary being the maximum margin hyperplane for learning samples (25). LR is a generalized linear model, in which logistic function is used for regression and classification (primarily 0/1 classification). The area analysis under the receiver operating characteristic (ROC) curve (AUC) was used to illustrate the predictive performance of radiomic characteristics. When the sensitivity and specificity were the largest, the optimal cut-off value was selected. A total of 4 indicators to evaluate the AUC and prediction accuracy of the training and validation sets. It includes P [accuracy=true positive/(true positive + false positive)]; R [recall rate=true positive/(true positive + false negative)]; F1 score [1 score=P * r * 2/(P + R)]; Support: to evaluate the performance of the classifier. $P<0.05$ was considered to indicate a statistically significant difference.

Results

A total of 381 ROIs (203 NTM pulmonary disease and 178 TB) were manually outlined (Fig. 1A and B) in the CT images of 192 patients (Table I). Computer-generated random numbers were utilized to assign 70% of ROI to the training data cohort and 30% to the verification data cohort. Using the variance threshold method, 456 features were selected for the models. Subsequently, best K method was employed in the selection of 315 features and then the LASSO algorithm was used to select 52 optimal features (Fig. 2). Of 52 radiomics features, 34 were texture analysis, one was shapes and 17 were first-order statistical feature groups. ROC curve analysis for both the training and validation cohort for differentiating between NTM pulmonary disease and TB is illustrated in Figs. 3 and 4.

Three classifiers were used to analyze the characteristics of the radiomic AUC; 95% CI, sensitivity and specificity of the training cohort and verification cohort are shown in Table II. In the training cohort, AUC [95% confidence interval (CI)], sensitivity and specificity of the KNN, SVM, and LR classifiers were 0.98 (0.95-1.00), 0.93 and 0.94, 0.99 (0.97-1.00), 0.96 and 0.96 and 0.99 (0.97-1.00), 0.97 and 0.97, respectively. In the validation cohort, these were 0.90 (0.82-0.97), 0.88 and 0.83, 0.92 (0.84-1.00), 0.86 and 0.85 and 0.89 (0.81-0.96), 0.88 and 0.85, respectively. In the external verification cohort, these were 0.84 (0.66-0.82), 0.65 and 0.83, 0.90 (0.78-0.92), 0.94 and 0.77 and 0.95 (0.84-0.96), 0.94 and 0.87, respectively. The ROC curves of the three classifiers are shown in Figs. 3 and 4. All cohorts had a significant AUC value >0.84.

In the training cohort, the precision of the three models was >0.94 and recall rate and F1 score were >0.93 (Table III). In the validation cohort, the precision of the three models was >0.83 with a recall rate and F1 score >0.86. Combining the precision, recall and F1 scores revealed that LR outperformed the other classifiers. In the external verification cohort, the precision of the three models was >0.77, the recall rate was >0.65 and F1 score was >0.69. LR classifier had the highest precision, recall and F1 score.

Table I. Allocation of ROIs to training, validation and external verification cohort.

ROIs	Total	Training cohort	Validation cohort	External verification cohort
NTM	203	124	32	47
TB	178	119	30	29

ROI, region of interest; NTM, non-tuberculous mycobacteria; TB, tuberculosis.

Discussion

NTM is a conditional pathogen caused by Mycobacteria other than *M. tuberculosis* complex and *Mycobacterium leprae*, which commonly exist in water and soil. A total of 191 species has been discovered, but only a few can cause disease (17,26-28). Individuals typically contract the disease via the environment, with water and soil being key (7,26,27). Additionally, the incidence rate of NTM pulmonary disease is increasing in United States, Germany, Canada and Taiwan (29-32). The clinical symptoms and pathology of NTM pulmonary disease are difficult to distinguish from TB and NTM is prone to natural drug resistance. The diagnosis of NTM pulmonary disease and TB is achieved via etiological detection. However, this is slow and complex, negatively impacting clinical treatment (17). In the misdiagnosis of NTM pulmonary disease as TB, the use of anti-TB treatment results in the delay of proper treatment, a prolonged course of disease, poor prognosis and possible treatment failure (33). Therefore, discovering simple and effective diagnostic methods is necessary.

Conventional CT is one of the primary detection methods for NTM pulmonary disease and pulmonary TB. However, CT manifestations of NTM pulmonary disease are complex and typically perceived as conditions such as consolidation, bronchiectasis, cavities and bronchial dissemination, which are difficult to distinguish from TB (34,35). Koh *et al* (36) discovered that bronchiolitis, consolidation and bronchiectasis can be perceived on CT images of NTM pulmonary disease, which often involve >5 lobes. If bronchiectasis involving the middle lobe of the right lung and the tongue segment of the upper lobe of the left lung is observed in CT images, along with cavities and nodules, NTM pulmonary disease should be considered (37). In some studies (11,15), probability of NTM consolidation is significantly lower than that of pulmonary TB. However, in other studies (12,34), the consolidation of conventional CT does not significantly differentiate NTM and TB.

Necrotizing granulomatous inflammation is the key characteristic lesion of tuberculosis, NTM pulmonary disease, Coccidiosis and cryptococcosis (37-41). NTM pulmonary disease is more prone to suppurative necrosis than TB, while pink and basophilic necrosis caused by TB are more common

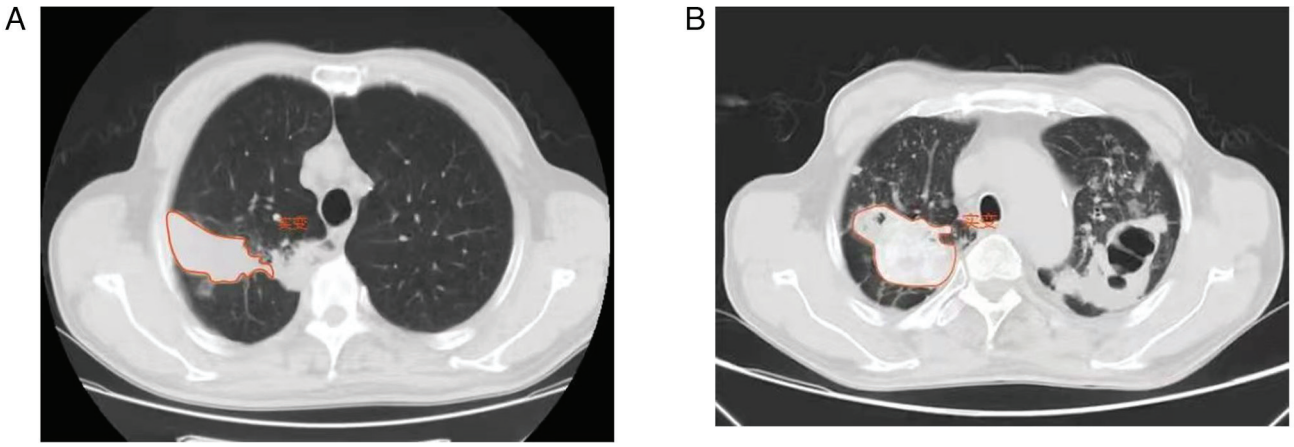

Figure 1. Region of interest (A) Male 63-year-old patient with a consolidation of NTM pulmonary disease in the right superior lobe. (B) Male 60-year-old patient with similar consolidation of PTB in the right superior lobe. NTM, non-tuberculous mycobacteria; PTB, pulmonary tuberculosis.

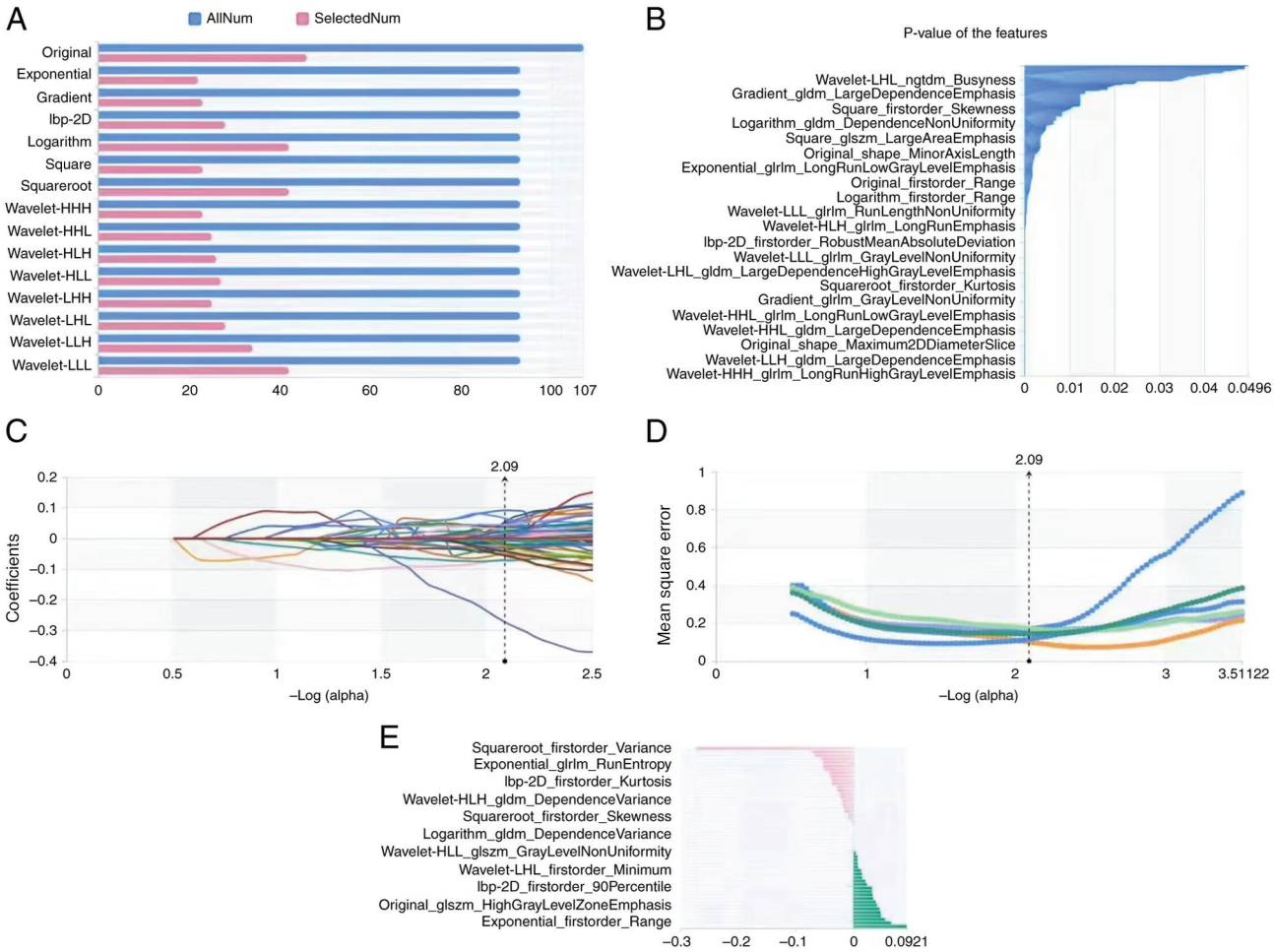

Figure 2. Radiomic feature extraction and selection. (A) Variance threshold was used to select 461 radiomics features (variance threshold=0.8) from 1,409 features. (B) Select K best was used to select 299 radiomics features. LASSO algorithm was used to select 63 features corresponding to the optimal α value. (C) LASSO path. (D) MSE path. (E) Coefficients in LASSO model. LASSO, least absolute shrinkage and selection operator; MSE, Mean Square Error.

than NTM pulmonary disease (42). NTM pulmonary disease possesses more giant or bizarre multinucleated giant cells compared with TB (43). The aggregation of epithelial-like cells leads to proliferative granuloma in NTM and caseous necrosis is less than that in TB (15). NTM pulmonary disease may result in atypical lesions, in which tissue cell aggregation with no granuloma is seen, which is common in immunodeficient patients (44,45). Consolidation of NTM pulmonary disease is less common than TB, with low incidence, less granuloma and more suppurative necrosis. It is difficult to observe differences

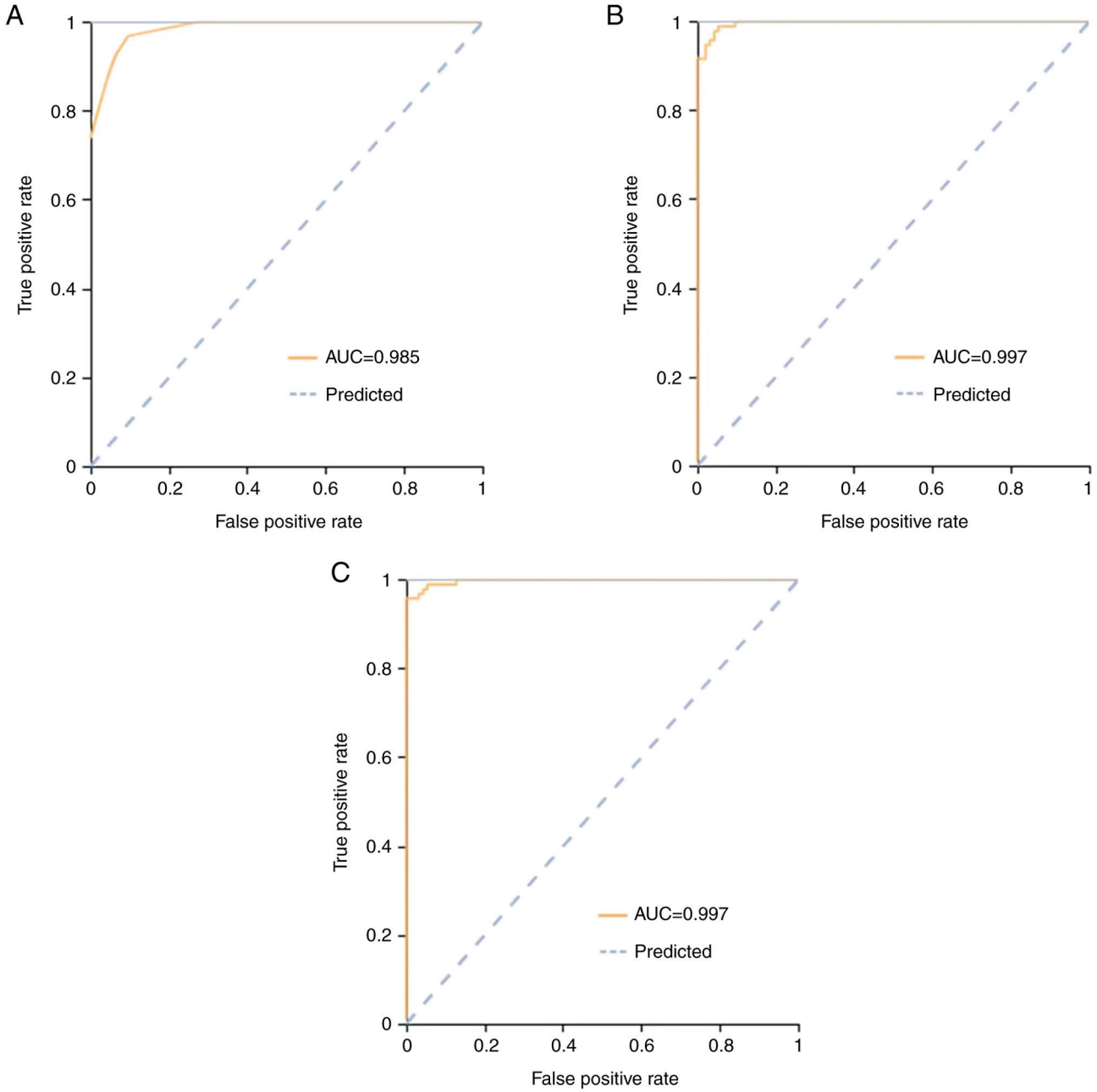

Figure 3. ROC curve of training cohort. ROC curves of (A) K-nearest neighbor, (B) Support vector machine and (C) Logistic regression classification. AUC, area under the curve; ROC, receiver operating characteristic.

in the pathological features of NTM and TB in conventional CT images, resulting in decreased differential diagnosis of TB.

Radiomics has developed substantially in recent years. Radiomics involves converting medical images into high-dimensional images, extracting data features through quantitative high-throughput and the analysis of the data for decision support (46). The sensitivity and predictive value of radiomics is significant in screening of small pulmonary nodules and diagnosis, treatment and prognosis of lung cancer (47-49). Radiomics may also detect common inflammatory lesions (50,51). Deep learning has been employed (25,52,53) to distinguish NTM pulmonary disease and TB, along with use of the cavity characteristics of radiomics to distinguish the two diseases. Consolidation features are common CT features of NTM pulmonary disease and TB. CT data extracted via high-throughput radiology reflect differences in the pathological characteristics of NTM and TB, compensating for fewer differences observed by the naked eye and the loss of information.

Here, consolidations of NTM pulmonary disease and TB were noted as ROIs. High-throughput image features were computed. A total of 52 radiomics features were obtained from the ROIs, of which 34 were texture analysis, one was shape and 17 were first-order statistical feature groups. Three supervised learning classifiers (KNN, SVM and LR) were used to analyze the extracted lung consolidation features. In the training cohort, the AUC values of models were all >0.98, 95% CI was 0.95-1.00, the sensitivity was >0.93 and the specificity was >0.94. In the validation cohort, the AUC values were all >0.89, 95% CI was 0.81-0.96, the sensitivity

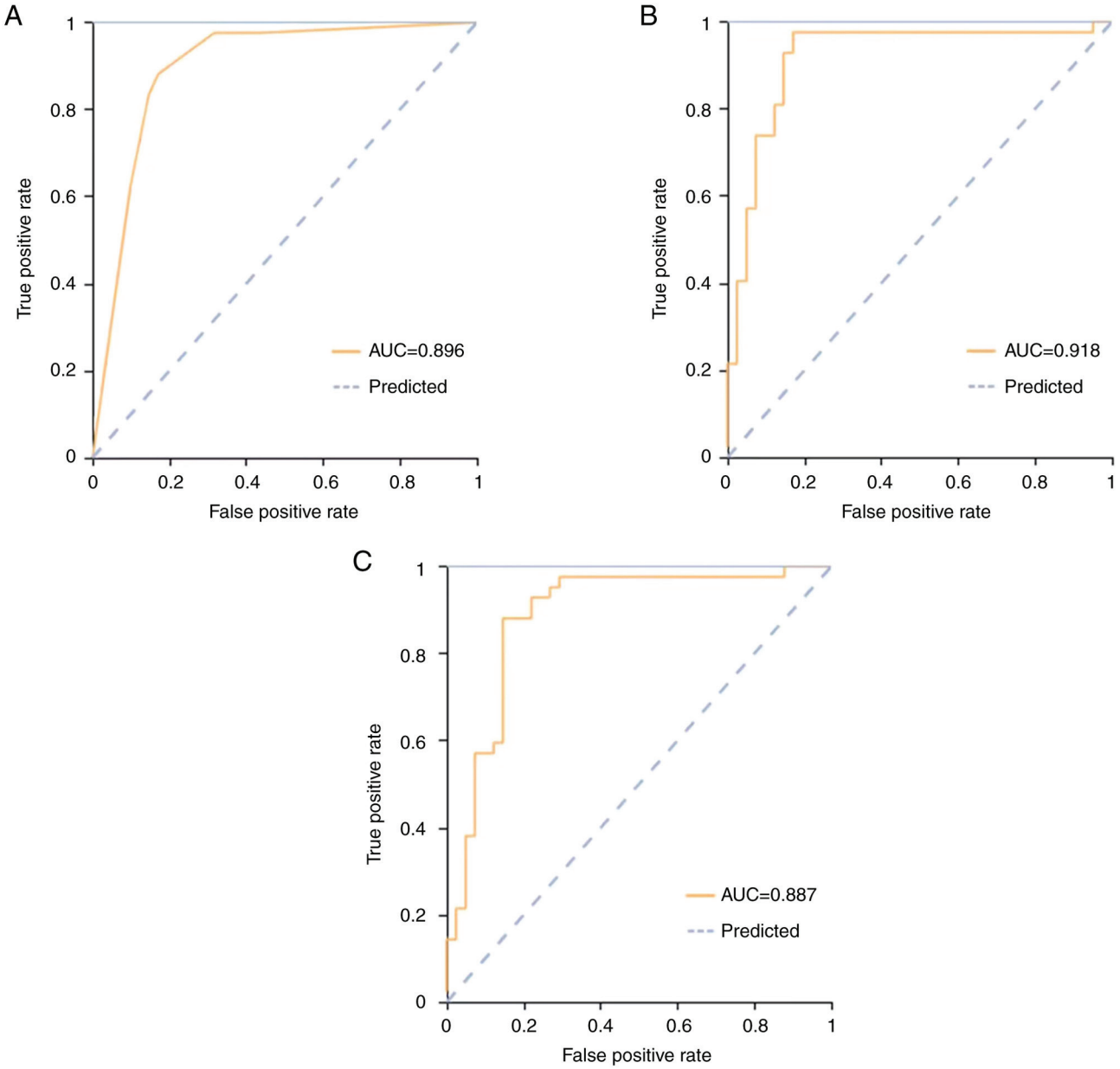

Figure 4. ROC curve of validation cohort. ROC curves of (A) K-nearest neighbor, (B) Support vector machine and (C) Logistic regression classification. AUC, area under the curve; ROC, receiver operating characteristic.

was >0.86 and the specificity was >0.83. AUC values of the ROC curve were all significant and their sensitivity and specificity as >0.83. In the external validation set, the AUC value was similar to that of internal validation set. In the present study, the characteristics of the classifiers were analyzed using clinical indicators (accuracy, recall, F1 score and support). The precision of models was >0.77, the recall rate was >0.65 and F1 score was >0.69. Further, the LR classifier yielded the highest precision, recall, and F1 score, which were >0.86, 0.87 and 0.87, respectively. From the results, it was observed that the radiomics features derived from consolidations held potential in differentiating between NTM pulmonary disease and TB. Although in some studies, the CT imaging characteristics of NTM pulmonary disease consolidations observed through traditional clinical methods differ from those of TB (16,40), results obtained by naked eye may be subjective. However, the present radiomics characteristics of consolidations have potential to distinguish between NTM pulmonary disease and TB. Radiomics analysis of consolidation characteristics of pulmonary diseases has the advantages of objectivity, quantification, stability and non-empirical dependence. Consequently, radiomics analysis possesses value in clinical application. Using radiomics characteristics to distinguish NTM pulmonary disease from TB is a promising, non-invasive and simple method. The early diagnosis of NTM pulmonary disease may improve the quality of life of patients and treatment of the disease, especially for resource-deficient medical systems in developing countries (54,55).

There are certain limitations to the present study. First, to ensure the homogeneity of the image, 5-mm-thick images were used, which may result in loss of information. Second,

Table II. Receiver operating characteristic results with KNN, SVM and LR classifiers.

A, Training cohort

Classifier	AUC	95% CI	Sensitivity	Specificity
KNN	0.98	0.95-1.00	0.93	0.94
SVM	0.99	0.97-1.00	0.96	0.96
LR	0.99	0.97-1.00	0.97	0.97

B, Validation cohort

Classifier	AUC	95% CI	Sensitivity	Specificity
KNN	0.90	0.82-0.97	0.88	0.83
SVM	0.92	0.84-1.00	0.86	0.85
LR	0.89	0.81-0.96	0.88	0.85

C, External validation cohort

Classifier	AUC	95% CI	Sensitivity	Specificity
KNN	0.84	0.66-0.82	0.65	0.83
SVM	0.90	0.78-0.92	0.94	0.77
LR	0.95	0.84-0.96	0.94	0.87

AUC, area under the curve; KNN, K-nearest neighbor; SVM, support vector machine; LR, logistic regression.

Table III. Precision, recall and F1 score.

	Training cohort			Validation cohort			External verification cohort		
Evaluation indicator	KNN	SVM	LR	KNN	SVM	LR	KNN	SVM	LR
Precision	0.94	0.96	0.97	0.83	0.85	0.85	0.83	0.77	0.87
Recall	0.93	0.96	0.97	0.88	0.86	0.88	0.65	0.94	0.94
F1 score	0.93	0.96	0.97	0.86	0.86	0.87	0.69	0.82	0.88

KNN, K-nearest neighbor; SVM, support vector machine; LR, logistic regression.

the sample size was small. Multicenter studies with larger sample sizes are required to validate the present results. ROI segmentation was performed manually, which may have been affected by subjective bias. Lastly, only consolidation was investigated and other characteristics were ignored, which may have resulted in incomplete information.

In the present study, radiomics features based on CT imaging were effective in identifying NTM pulmonary disease and TB consolidation. Additionally, LR classifier outperformed the other classifiers in the recognition of consolidation of NTM pulmonary disease in patients.

Acknowledgements

Not applicable.

Funding

The present study was supported by Shandong Medical and Health Science and Technology Development Plan Project (grant no. 2019WS535).

Availability of data and materials

The datasets used and/or analysed during the current study are available from the corresponding author on reasonable request.

Authors' contributions

QY, WZ and DY made substantial contributions to conception and design. QY, JCu and JCh made substantial contributions

to acquisition of data. JCu, HK, JCh and ZD made substantial contributions to analysis and interpretation of data. QY and ZD wrote the manuscript. HK and JCu constructed figures. JCh and JCu constructed tables. All authors have read and approved the final manuscript. QY and JCu confirm the authenticity of all the raw data.

Ethics approval and consent to participate

The present study was approved by the ethics committee of Shandong Public Health Clinical Center (Shandong Provincial Chest Hospital) and the requirement for consent for this retrospective analysis was waived (approval no. 2019XKYYEC-29).

Patient consent for publication

Not applicable.

Competing interests

The authors declare that they have no competing interests.

References

1. Marshall JE, Mercaldo RA, Lipner EM and Prevots DR: Incidence of nontuberculous mycobacteria infections among persons with cystic fibrosis in the United States (2010-2019). BMC Infect Dis 23: 489, 2023.
2. Dahl VN, Fløe A and Wejse C: Nontuberculous mycobacterial infections in a Danish region between 2011 and 2021: Evaluation of trends in diagnostic codes. Infect Dis (Lond) 55: 439-443, 2023.
3. Khan K, Wang J and Marras TK: Nontuberculous mycobacterial sensitization in the United States: National trends over three decades. Am J Respir Crit Care Med 176: 306-313, 2007.
4. Khan K, Wang J, Hu W, Bierman A, Li Y and Gardam M: Tuberculosis infection in the United States: National trends over three decades. Am J Respir Crit Care Med 177: 455-460, 2008.
5. Marras TK, Chedore P, Ying AM and Jamieson F: Isolation prevalence of pulmonary non-tuberculous mycobacteria in Ontario, 1997 2003. Thorax 62: 661-666, 2007.
6. Thornton CS, Mellett M, Jarand J, Barss L, Field SK and Fisher DA: The respiratory microbiome and nontuberculous mycobacteria: An emerging concern in human health. Eur Respir Rev 30: 200299, 2021.
7. Chinese Medical Association Tuberculosis Branch, Editorial Board of Chinese Journal of Tuberculosis and Respiratory Medicine: Expert consensus on diagnosis and treatment of nontuberculous mycobacterial disease. Chin J Tubercul Respir Dis 35: 572-580, 2012.
8. Gopalaswamy R, Shanmugam S, Mondal R and Subbian S: Of tuberculosis and non-tuberculous mycobacterial infections-a comparative analysis of epidemiology, diagnosis and treatment. J Biomed Sci 27: 74, 2020.
9. Cao P, Liu F and Li H: Clinical analysis of 58 cases of non-tuberculous mycobacteria. Chongqing Med J 43: 854-856, 2014 (In Chinese).
10. Chu HQ, Li B, Zhao L, Huang DD, Zhang ZM, Xu JF, Zhang JB, Gui T, Xu LY and Sun XW: Chest imaging comparison between non-tuberculous and tuberculosis mycobacteria in sputum acid fast bacilli smear-positive patients. Eur Rev Med Pharmacol Sci 19: 2429-2439, 2015.
11. You Z and Zhu X: CT findings of pulmonary nontuberculous mycobacterial disease. Chin J Clin Med Imaging 16: 141-143, 2005.
12. Dai J Shi J and Liang L: Comparison of CT findings between non tuberculous mycobacterial lung disease and secondary pulmonary tuberculosis. Chin J Tubercul 36: 706-709, 2014.
13. Ma J, Zhou Z, Ren Y, Xiong J, Fu L, Wang Q and Zhao J: Computerized detection of lung nodules through radiomics. Med Phys 44: 4148-4158, 2017.
14. Coroller TP, Agrawal V, Huynh E, Narayan V, Lee SW, Mak RH and Aerts HJWL: Radiomic-based pathological response prediction from primary tumors and lymph nodes in NSCLC. J Thorac Oncol 12: 467-476, 2017.
15. Wittram C and Weisbrod GL: Mycobacterium avium complex lung disease in immunocompetent patients: Radiography-CT correlation. Br J Radiol 75: 340-344, 2002.
16. Guo H: To explore the clinical value of CT in the diagnosis and clinicopathological classification of peripheral small lung cancer. China Contin Med Educ 8: 48, 2016 (In Chinese).
17. Daley CL, Iaccarino JM, Lange CG, Cambau E, Wallace RJ Jr, Andrejak C, Böttger EC, Brozek J, Griffith DE, Guglielmetti L, *et al*: Treatment of nontuberculous mycobacterial pulmonary disease: An official ATS/ERS/ESCMID/IDSA clinical practice guideline. Eur Respir J 56: 2000535, 2020.
18. Liu E, Zhou L and Wang L: Comprehensively interpret the standards of 'ws 196-2017 tuberculosis classification. Chin J Tubercul Prev 40: 5, 2018 (In Chinese).
19. Wang Y, Lu B, Liu J, Xiao T, Wan K and Guan C: A multicenter clinical evaluation of *Mycobacterium tuberculosis* IgG/IgM antibody detection using the colloidal gold method. Eur J Clin Microbiol Infect Dis 33: 1989-1994, 2014.
20. Lambin P, Rios-Velazquez E, Leijenaar R, Carvalho S, van Stiphout RG, Granton P, Zegers CM, Gillies R, Boellard R, Dekker A and Aerts HJ: Radiomics: Extracting more information from medical images using advanced feature analysis. Eur J Cancer 48: 441-446, 2012.
21. Akman DV, Malekipirbazari M, Yenice ZD, Yeo A, Adhikari N, Wong YK, Abbasi B and Gumus AT: K-best feature selection and ranking via stochastic approximation. Expert Syst Appl 213: 118864, 2023.
22. Choi H, Song E, Hwang SS and Lee W: A modified generalized lasso algorithm to detect local spatial clusters for count data. AStA Adv Stat Anal 102: 537-563, 2018.
23. Sun H, Zhou P, Chen G, Dai Z, Song P and Yao J: Radiomics nomogram for the prediction of Ki-67 index in advanced non-small cell lung cancer based on dual-phase enhanced computed tomography. J Cancer Res Clin Oncol 149: 9301-9315, 2023.
24. Hapsari DP, Utoyo I and Purnami SW: Support vector machine optimization with fractional gradient descent for data classification. J Appl Sci Manag Eng Technol 2: 1-6, 2021.
25. Zhou Z: Machine learning. Tsinghua University Press, pp121-139, 298-300, 2016.
26. Wang L, Ding W, Mo Y, Shi D, Zhang S, Zhong L, Wang K, Wang J, Huang C, Zhang S, *et al*: Distinguishing nontuberculous mycobacteria from *Mycobacterium tuberculosis* lung disease from CT images using a deep learning framework. Eur J Nucl Med Mol Imaging 8: 4293-4306, 2021.
27. Biondi G, Sotgiu G, Dore S, Molicotti P, Ruggeri M, Aliberti S and Satta R: Beyond pulmonary nontuberculous mycobacteria disease: Do extra-pulmonary forms represent an emerging clinical and public health threat? ERJ Open Res 3: 00091-2017, 2017.
28. Aboagye SY, Danso E, Ampah KA, Nakobu Z, Asare P, Otchere ID, Röltgen K, Yirenya-Tawiah D and Yeboah-Manu D: Isolation of nontuberculous mycobacteria from the environment of ghanian communities where buruli ulcer is endemic. Appl Environ Microbiol 82: 4320-4329, 2016.
29. Chen CY, Chen HY, Chou CH, Huang CT, Lai CC and Hsueh PR: Pulmonary infection caused by nontuberculous mycobacteria in a medical center in Taiwan, 2005-2008. Diagn Microbiol Infect Dis 72: 47-51, 2012.
30. Vinnard C, Longworth S, Mezochow A, Patrawalla A, Kreiswirth BN and Hamilton K: Deaths related to nontuberculous mycobacterial infections in the United States, 1999-2014. Ann Am Thorac Soc 13: 1951-1955, 2016.
31. Ringshausen FC, Wagner D, de Roux A, Diel R, Hohmann D, Hickstein L, Welte T and Rademacher J: Prevalence of nontuberculous mycobacterial pulmonary disease, Germany, 2009-2014. Emerg Infect Dis 22: 1102-1105, 2016.
32. Marras TK, Campitelli MA, Lu H, Chung H, Brode SK, Marchand-Austin A, Winthrop KL, Gershon AS, Kwong JC and Jamieson FB: Pulmonary nontuberculous mycobacteria-associated deaths, Ontario, Canada, 2001-2013. Emerg Infect Dis 23: 468-476, 2017.
33. Jing H, Wang H, Wang Y, Deng Y, Li X, Liu Z, Graviss EA and Ma X: Prevalence of nontuberculous mycobacteria infection, China, 2004-2009. Emerg Infect Dis 18: 527-528, 2012.

34. Eisenberg I, Yasin A, Fuks L, Stein N, Saliba W, Kramer MR, Adir Y and Shteinberg M: Radiologic characteristics of non-tuberculous mycobacteria infection in patients with bronchiectasis. Lung 198: 715-722, 2020.
35. Kwak N, Lee JH, Kim HJ, Kim SA and Yim JJ: New-onset nontuberculous mycobacterial pulmonary disease in bronchiectasis: Tracking the clinical and radiographic changes. BMC Pulm Med 20: 293, 2020.
36. Koh WJ, Lee KS, Kwon OJ, Jeong YJ, Kwak SH and Kim TS: Bilateral bronchiectasis and bronchiolitis at thin-section CT: Diagnostic implications in nontuberculous mycobacterial pulmonary infection. Radiology 235: 282-288, 2005.
37. Aksamit TR, Philley JV and Griffith DE: Nontuberculous mycobacterial (NTM) lung disease: The top ten essentials. Respir Med 108: 417-425, 2014.
38. Marchevsky A, Damsker B, Gribetz A, Tepper S and Geller SA: The spectrum of pathology of nontuberculous mycobacterial infections in open-lung biopsy specimens. Am J Clin Pathol 78: 695-700, 1982.
39. Goodwin RA Jr and Snell JD Jr: The enlarging histoplasmoma. Concept of a tumor-like phenomenon encompassing the tuberculoma and coccidioidoma. Am Rev Respir Dis 100: 1-12, 1969.
40. Mukhopadhyay S and Gal AA: Granulomatous lung disease: An approach to the differential diagnosis. Arch Pathol Lab Med 134: 667-690, 2010.
41. Mukhopadhyay S: Role of histology in the diagnosis of infectious causes of granulomatous lung disease. Curr Opin Pulm Med 17: 189-196, 2011.
42. Mu J, Liu Z and Zhang C: Pathological characteristics of nontuberculous *Mycobacterium tuberculosis* and the value of molecular pathology in its diagnosis. Chin J Pathol 49: 562-567, 2020.
43. O'Leary S, O'Sullivan MP and Keane J: IL-10 blocks phagosome maturation in *Mycobacterium tuberculosis*-infected human macrophages. Am J Respir Cell Mol Biol 45: 172-180, 2011.
44. Jannotta FS and Sidawy MK: The recognition of mycobacterial infections by intraoperative cytology in patients with acquired immunodeficiency syndrome. Arch Pathol Lab Med 113: 1120-1123, 1989.
45. Marinelli DL, Albelda SM, Williams TM, Kern JA, Iozzo RV and Miller WT: Nontuberculous mycobacterial infection in AIDS: Clinical, pathologic, and radiographic features. Radiology 160: 77-82, 1986.
46. de la Pinta C: Radiomics in pancreatic cancer for oncologist: Present and future. Hepatobiliary Pancreat Dis Int 21: 356-361, 2022.
47. Gulshan V, Peng L, Coram M, Stumpe MC, Wu D, Narayanaswamy A, Venugopalan S, Widner K, Madams T, Cuadros J, *et al*: Development and validation of a deep learning algorithm for detection of diabetic retinopathy in retinal fundus photographs. JAMA 316: 2402-2410, 2016.
48. Chae HD, Park CM, Park SJ, Lee SM, Kim KG and Goo JM: Computerized texture analysis of persistent part-solid ground-glass nodules: Differentiation of preinvasive lesions from invasive pulmonary adenocarcinomas. Radiology 273: 285-293, 2014.
49. Liu Y, Kim J, Balagurunathan Y, Li Q, Garcia AL, Stringfield O, Ye Z and Gillies RJ: Radiomic features are associated with EGFR mutation status in lung adenocarcinomas. Clin Lung Cancer 17: 441-448.e6, 2016.
50. Zhang T, Yuan M, Zhong Y, Zhang YD, Li H, and Wu JF: Differentiation of focal organising pneumonia and peripheral adenocarcinoma in solid lung lesions using thin-section CT-based radiomics. Clin Radiol 74: 78.e23-78.e30, 2019.
51. Yanling W, Duo G, Zuojun G, Zhongqiang S, Yankai W, Shan L and Hongying C: Radiomics nomogram analyses for differentiating pneumonia and acute paraquat lung injury. Sci Rep 9: 15029, 2019.
52. Yan Q, Wang W, Zhao W, Zuo L, Wang D, Chai X and Cui J: Differentiating nontuberculous mycobacterium pulmonary disease from pulmonary tuberculosis through the analysis of the cavity features in CT images using radiomics. BMC Pulm Med 22: 4, 2022.
53. Xing Z, Ding W, Zhang S, Zhong L, Wang L, Wang J, Wang K, Xie Y, Zhao X, Li N and Ye Z: Machine learning-based differentiation of nontuberculous mycobacteria lung disease and pulmonary tuberculosis using CT images. Biomed Res Int 2020: 6287545, 2020.
54. Tan Y, Su B, Shu W, Cai X, Kuang S, Kuang H, Liu J and Pang Y: Epidemiology of pulmonary disease due to nontuberculous mycobacteria in Southern China, 2013-2016. BMC Pulm Med 18: 168, 2018.
55. Maurya AK, Nag VL, Kant S, Kushwaha RAS, Kumar M, Singh AK and Dhole TN: Prevalence of nontuberculous mycobacteria among extrapulmonary tuberculosis cases in tertiary care centers in Northern India. Biomed Res Int 2015: 465403, 2015.